Joint inversion of PP- wave and PSV- wave data for P- wave and S- wave inverse quality factors at different frequencies — Synthetic test

Huaizhen Chen, Kristopher Innanen, Yuxin Ji(SINOPEC), Xiucheng Wei

ABSTRACT

P- wave and S- wave quality factors (Q_{P} and Q_{S}) can provide valuable information for identifying the type of fluid in reservoir space. The results calculated by rock physics attenuation model suggest that P- wave and S- wave velocities (V_{P} and V_{S}) and quality factors vary with frequency, which also induce the reflection amplitude variation with frequency. However, the variation of velocities with frequency is small within the seismic frequency range, which can be ignored in the approximation of PP- wave and PSV- wave reflection coefficients. Our research begins with the rock physics numerical modeling to verify the reliability of ignoring the influence of frequency on velocities. The reflection coefficient approximate formulas of PP- wave and PSV- wave are derived using scattering function, and these formulas can be applied in the inversion of seismic data for elastic properties (P-wave and S- wave impedances and density) and quality factors. PP- wave and PSV- wave are employed in our approach to estimate quality factors, which can help to improve the accuracy of the inversion. Singular value decomposition (SVD) algorithm is used to solve the inversion problem, and initial models are utilized to constraint the inversion. Synthetic tests show the P- wave and S- wave impedances, density and inverse quality factors can be estimated reasonably even in the case that signal-to-noise ratio (SNR) is 2.

INTRODUCTION

Rock physics studies show that quality factors are influenced by reservoir parameters (porosity, fluid type, saturation, frequency etc.). Boit (1956) derived some equations for expressing the frequency dependent velocities. In his equations, the quality factor is related to the mechanisms of viscous and inertial interaction between the pore fluid and the mineral matrix of the rock. Dvorkin et al. (1995) introduced a model for calculating the elastic properties and attenuations at any intermediate frequency, and in their model, P- wave and S- wave quality factors (Q_{P} and Q_{S}) are expressed as the ratios of the absolute value of the real part to the imaginary part of P- wave and shear moduli, respectively. Using their model, we can model the influence of some reservoir parameters on quality factors.

In a viscoelastic medium, the complex P- wave and S- wave velocities (V_{P} and V_{S}) are functions of quality factors and the elastic velocities (V_{PE} and V_{SE}), and the complex velocities can induce the complex reflectivities. Recent studies, such as those of Innanen (2011), Bird (2012), Moradi and Innanen (2015) and Zong et al. (2005), have shown that the reflection coefficient of the viscoelastic medium can be expressed in terms of the reflectivities of P- wave velocity (V_{PE}), S- wave velocity (V_{SE}), and density (ρ), and quality factors. Following Moradi and Innanen (2015), we derive PP- wave and PSV- wave reflection approximate coefficients for the homogenous viscoelastic medium.

Joint inversion of PP- wave and PSV- wave seismic data has been proved to be a useful

tool to estimate the elastic properties (Stewart, 1990; Larsen, 1999; Margrave et al., 2001). In order to improve the accuracy of the estimation of elastic properties and quality factors, in the present research, we demonstrate a joint inversion method to estimate P- wave and S- wave impedances, density, and inverse quality factors, and the singular value decomposition (SVD) algorithm is employed to solve the inversion problem. Initial models are used to constrain the inversion. Synthetic data, which are added with different signal-to-noise (SNR) ratio noises, are used to verify our inversion approach.

THEORETICAL BACKGROUND

The expression of complex stiffness perturbation

The propagation factors for the elastic and viscoelastic media are respectively given by Aki and Richards (2002) as

$$\exp[i(kx - \omega t)] = \exp[i\omega(\frac{x}{V_e} - t)], \tag{1}$$

$$\exp[i(Kx - \omega t)] = \exp[\frac{-\omega x}{2V(\omega)Q(\omega)}]\exp[\frac{i\omega x}{V(\omega)} - i\omega t], \tag{2}$$

where k and K are the complex wave parameters for the elastic and viscoelastic media, ω is the angular frequency, V_e is the velocity for the elastic medium, $V(\omega)$ and $Q(\omega)$ are frequency-dependent velocity and quality factor for the viscoelastic medium respectively.

Comparing equation 1 with equation 2, the complex velocity V for the viscoelastic medium is expressed, to first order, as

$$V_{visco} = V(\omega)[1 - \frac{i}{2Q(\omega)}], \tag{3}$$

The complex P- wave and S- wave velocities, V_{P} and V_{S}, are given by

$$V_{\mathrm{P}-visco} = V_{\mathrm{P}}(\omega)[1 - \frac{i}{2Q_{\mathrm{P}}(\omega)}], \tag{4}$$

$$V_{\mathrm{S}-visco} = V_{\mathrm{S}}(\omega)[1 - \frac{i}{2Q_{\mathrm{S}}(\omega)}], \tag{5}$$

Under the assumption that the attenuation is mainly induced by the interaction between the pore fluid and the mineral matrix of the rock, we use the extension of Mavko-Jizba squirt model for all frequencies (Dvorkin et al., 1995; Mavko et al., 2009) to generate the P- wave and S- wave velocities and quality factors variations with frequency and rock property (porosity and fluid), as shown in Figure 1 and Figure 2.

Some constants in the Mavko-Jizba squirt model we use are that Z value is 0.08, pore aspect ratio is 0.1, and the effective bulk modulus of dry rock at very high pressure is 50 GPa. We can see that the P- wave attenuation ($1/Q_{\mathrm{P}}$) increases with the porosity and gas

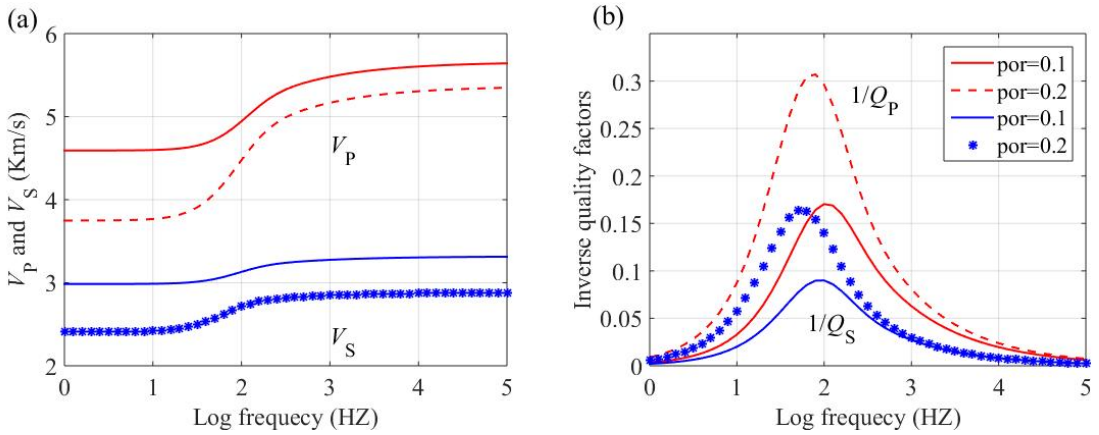

FIG. 1. P- and S- wave velocities and quality factors variations with frequency and rock porosity (The water saturation is 1).

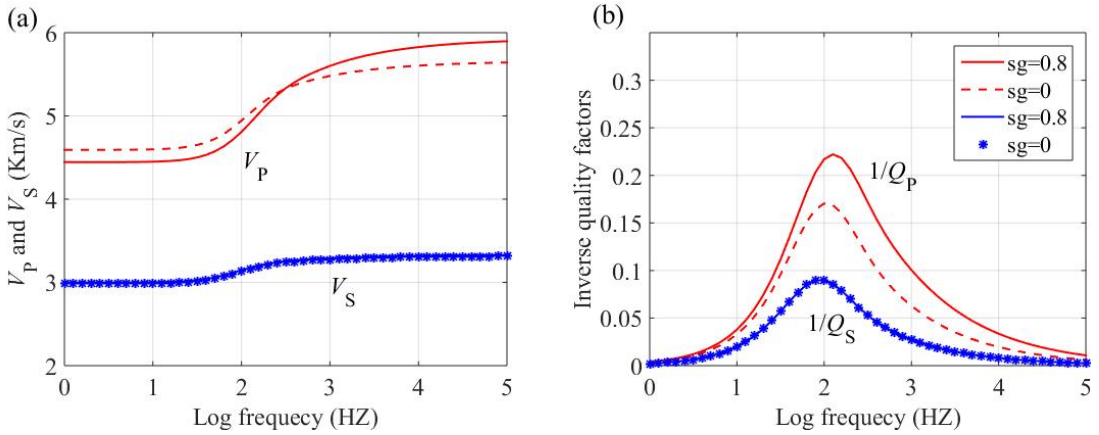

FIG. 2. P- and S- wave velocities and quality factors variations with frequency and gas saturation (The porosity is 0.1, and the fluid is the mixture of gas and water).

saturation, and S- wave attenuation ($1/Q_{\rm S}$) increases with the porosity and has no change with the fluid saturation. The variations of P- wave and S- wave velocities and quality factors indicate that the influence of frequency should not be ignorable.

From equations 4 and 5, the complex stiffness parameters $C_{33-visco}$ and $C_{55-visco}$ of viscoelastic media are expressed as (ignoring the high order of $Q_{\rm P}$ and $Q_{\rm S}$)

$$C_{33-visco} = \rho[V_{\rm P}(\omega)]^2[1 - \frac{i}{2Q_{\rm P}(\omega)}]^2 \approx C_{33}(\omega)[1 - \frac{i}{Q_{\rm P}(\omega)}], \tag{6}$$

$$C_{55-visco} = \rho[V_{\rm S}(\omega)]^2[1 - \frac{i}{2Q_{\rm S}(\omega)}]^2 \approx C_{55}(\omega)[1 - \frac{i}{Q_{\rm S}(\omega)}], \tag{7}$$

The perturbation of complex stiffness parameters, $\Delta C_{33-visco}$ and $\Delta C_{55-visco}$, are expressed as

$$\Delta C_{33_{-visco}} = \Delta C_{33}(\omega)[1 - \frac{i}{Q_{\rm P}(\omega)}] + C_{33}(\omega)\frac{\Delta Q_{\rm P}(\omega)}{[Q_{\rm P}(\omega)]^2}, \tag{8}$$

$$\Delta C_{55_{-visco}} = \Delta C_{55}(\omega)[1 - \frac{i}{Q_{\rm S}(\omega)}] + C_{55}(\omega)\frac{\Delta Q_{\rm S}(\omega)}{[Q_{\rm S}(\omega)]^2}, \tag{9}$$

The perturbation of complex stiffness matrix in the viscoelastic medium is expressed as

$$\Delta C_{visco} = \begin{bmatrix} \Delta C_{33-visco} & \Delta C_{12-visco} & \Delta C_{12-visco} & 0 & 0 & 0 \\ \Delta C_{12-visco} & \Delta C_{33-visco} & \Delta C_{12-visco} & 0 & 0 & 0 \\ \Delta C_{12-visco} & \Delta C_{12-visco} & \Delta C_{33-visco} & 0 & 0 & 0 \\ 0 & 0 & 0 & \Delta C_{55-visco} & 0 & 0 \\ 0 & 0 & 0 & 0 & \Delta C_{55-visco} & 0 \\ 0 & 0 & 0 & 0 & 0 & \Delta C_{55-visco} \end{bmatrix}, \tag{10}$$

where $\Delta C_{12-visco} = \Delta C_{33-visco} - 2\Delta C_{55-visco}$.

Linearized PP- wave and PSV- wave reflection coefficients

Under the assumption of Born integral and stationary phase, Shaw and Sen (2004, 2006) derived the linearized equations to calculate PP- wave and PSV- wave reflection coefficients

$$R_{\rm PP} = \frac{1}{4\rho \cos^2\theta} S, \tag{11}$$

$$R_{\rm PS} = \frac{\sin\theta}{2\rho \cos\varphi \sin(\theta + \varphi)} S, \tag{12}$$

where ρ is the density of the reference elastic medium, S is the scattering function, θ is the P- wave incident angle, φ is the S- wave incident angle, and $\sin\varphi = \frac{\beta}{\alpha}\sin\theta$.

Following Shaw and Sen (2004, 2006), we derive the approximate expressions of the complex PP- wave and PSV- wave reflection coefficients for the homogeneous viscoelastic medium based on their proposed expression of the scattering function

$$S = \Delta\rho\xi + \Delta C_{\rm mn}\eta_{\rm mn}, \tag{13}$$

where $\xi = \mathrm{g}_i \mathrm{g}_i^{'}$ and $\eta_{\mathrm{mn}} = \mathrm{g}_i^{'} \mathrm{p}_j^{'} \mathrm{g}_k \mathrm{p}_l$. In addition, p and g are the slowness and polarization parameters, $\Delta\rho$ is the perturbation of density, and ΔC_{mn} is the perturbation of complex stiffness matrix (i.e. equation 10).

For the case of azimuth ϕ being zero, the PP- wave and PSV- wave reflection coefficients are expressed as

$$\begin{aligned} R_{\mathrm{PP}}(\theta,\omega) = \sec^2\theta R_{\mathrm{P}}(\omega) - 8g\sin^2\theta R_{\mathrm{S}}(\omega) + (4g\sin^2\theta - \tan^2\theta) R_{\mathrm{D}} \\ -\sec^2\theta [R_{\mathrm{P}}(\omega) - \frac{1}{2} R_{\mathrm{D}}] \frac{i}{Q_{\mathrm{P}}(\omega)} + \frac{1}{4}\sec^2\theta \frac{\Delta Q_{\mathrm{P}}(\omega)}{Q_{\mathrm{P}}(\omega)} \frac{i}{Q_{\mathrm{P}}(\omega)} \\ +4g\sin^2\theta [2R_{\mathrm{S}}(\omega) - R_{\mathrm{D}}] \frac{i}{Q_{\mathrm{S}}(\omega)} - 2g\sin^2\theta \frac{\Delta Q_{\mathrm{S}}(\omega)}{Q_{\mathrm{S}}(\omega)} \frac{i}{Q_{\mathrm{S}}(\omega)}, \end{aligned} \tag{14}$$

$$\begin{aligned} R_{\mathrm{PSV}}(\varphi,\omega) = -4\frac{\sin\theta}{\cos\varphi}(\sqrt{g}\cos\theta\cos\varphi - g\sin^2\theta) R_{\mathrm{S}}(\omega) \\ +\frac{\sin\theta}{\cos\varphi}(2\sqrt{g}\cos\theta\cos\varphi - 2g\sin^2\theta - 1) R_{\mathrm{D}} \\ +2\frac{\sin\theta}{\cos\varphi}(\sqrt{g}\cos\theta\cos\varphi - g\sin^2\theta)[2R_{\mathrm{S}}(\omega) - R_{\mathrm{D}}] \frac{i}{Q_{\mathrm{S}}(\omega)} \\ -\frac{\sin\theta}{\cos\varphi}(\sqrt{g}\cos\theta\cos\varphi - g\sin^2\theta) \frac{\Delta Q_{\mathrm{S}}(\omega)}{Q_{\mathrm{S}}(\omega)} \frac{i}{Q_{\mathrm{S}}(\omega)}, \end{aligned} \tag{15}$$

where $R_{\mathrm{P}}(\omega) = \dfrac{\Delta I_{\mathrm{P}}(\omega)}{I_{\mathrm{P}}(\omega)} = \dfrac{\Delta\alpha(\omega)}{2\alpha(\omega)} + \dfrac{\Delta\rho}{2\rho}$, $R_{\mathrm{S}}(\omega) = \dfrac{\Delta I_{\mathrm{S}}(\omega)}{I_{\mathrm{S}}(\omega)} = \dfrac{\Delta\beta(\omega)}{2\beta(\omega)} + \dfrac{\Delta\rho}{2\rho}$, and $R_{\mathrm{D}} = \dfrac{\Delta\rho}{2\rho}$. For the case of constant Q, $V_{\mathrm{P}}(\omega) = V_{\mathrm{P}}(\omega_r)[1 + \dfrac{1}{\pi Q_{\mathrm{P}}} log(\dfrac{\omega}{\omega_r})]$, and $V_{\mathrm{S}}(\omega) = V_{\mathrm{S}}(\omega_r)[1 + \dfrac{1}{\pi Q_{\mathrm{S}}} log(\dfrac{\omega}{\omega_r})]$ (Aki and Richards, 2002). In addition, ω_r is the reference frequency.

We construct an effective model (an elastic medium over a viscoelastic medium, Figure 3) to calculate PP- wave and PSV- wave reflection coefficients at different frequencies. Elastic parameters of the upper layer of the effective model, P- wave and S- wave velocities, and density, are from the shale-gas sand model (Goodway et al., 1997), and the inverse quality factors are zero. Reservoir parameters of the lower layer are shown in Figure 3.

In the present study, we use the extension of Mavko-Jizba squirt model to calculate P-wave and S- wave velocities and inverse quality factors for the case of gas-filled (gas saturation, Sg, is 1) lower layer at different frequencies. Figure 4 shows the real and imaginary parts of PP- wave and PSV- wave reflection coefficients. We can see that real parts of PP-wave and PSV- wave reflection coefficients variations with frequency are small in seismic frequency range, the imaginary parts are smaller than the real parts, and the imaginary parts vary with frequency obviously.

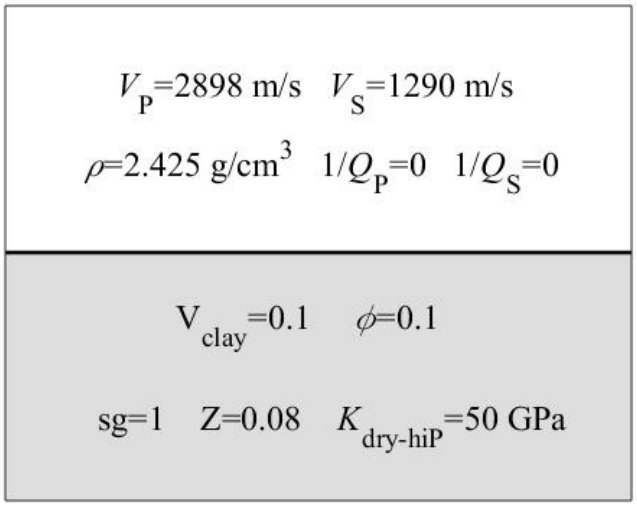

FIG. 3. The elastic medium over viscoelastic medium model.

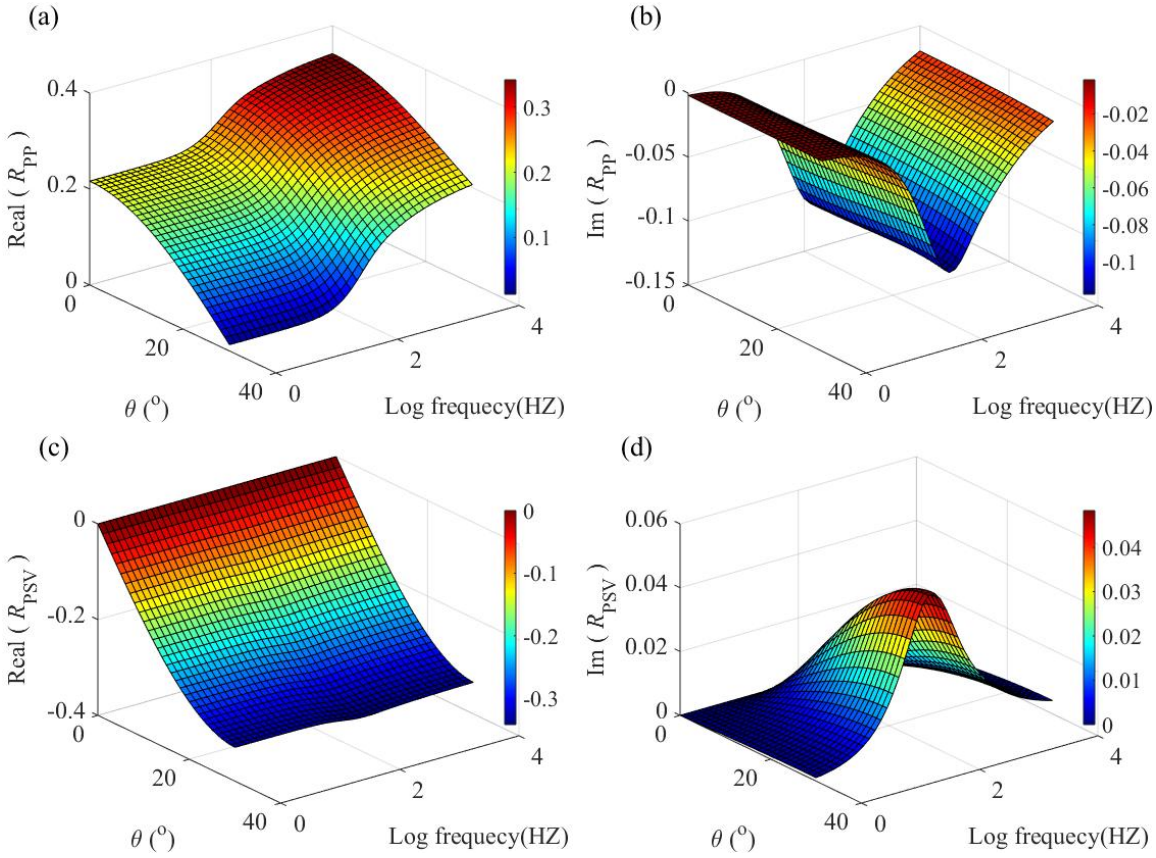

FIG. 4. Complex PP- wave and PSV- wave reflection coefficients. (a) Real part of PP- wave reflection coefficient; (b) Imaginary part of PP- wave reflection coefficient; (c) Real part of PSV-wave reflection coefficient; (d) Imaginary part of PSV-wave reflection coefficient.

Joint PP- wave and PSV- wave inversion for inverse quality factors

For a highly attenuative reservoir (the overlying and underlying layers are elastic, $\frac{\Delta Q_{\rm P}(\omega)}{Q_{\rm P}^2(\omega)} \approx \frac{1}{Q_{\rm P}(\omega)}$ and $\frac{\Delta Q_{\rm S}(\omega)}{Q_{\rm S}^2(\omega)} \approx \frac{1}{Q_{\rm S}(\omega)}$), we simplify PP- wave and PSV- wave reflection coefficients as

$$\begin{aligned} R_{\rm PP}(\theta,\omega) &= \sec^2\theta R_{\rm P}(\omega) - 8g\sin^2\theta R_{\rm S}(\omega) + (4g\sin^2\theta - \tan^2\theta)R_{\rm D} \\ -\sec^2\theta[R_{\rm P}(\omega) - \frac{1}{2}R_{\rm D} - \frac{1}{4}]\frac{i}{Q_{\rm P}(\omega)} &+ 4g\sin^2\theta[2R_{\rm S}(\omega) - R_{\rm D} - \frac{1}{2}]\frac{i}{Q_{\rm S}(\omega)}. \end{aligned} \tag{16}$$

$$\begin{aligned} R_{\rm PSV}(\varphi,\omega) &= -4\frac{\sin\theta}{\cos\varphi}(\sqrt{g}\cos\theta\cos\varphi - g\sin^2\theta)R_{\rm S}(\omega) \\ &+\frac{\sin\theta}{\cos\varphi}(2\sqrt{g}\cos\theta\cos\varphi - 2g\sin^2\theta - 1)R_{\rm D} \\ +2\frac{\sin\theta}{\cos\varphi}(\sqrt{g}\cos\theta\cos\varphi - g\sin^2\theta)&[2R_{\rm S}(\omega) - R_{\rm D} - \frac{1}{2}]\frac{i}{Q_{\rm S}(\omega)}. \end{aligned} \tag{17}$$

Since equations (16) and (17) are derived in the frequency domain, the synthetic seismic are generated by

$$\begin{aligned} S_{\rm PP}(\theta,\omega) &= a(\theta)W(\omega)R_{\rm P} + b(\theta)W(\omega)R_{\rm S} + c(\theta)W(\omega)R_{\rm D} \\ &+d(\theta)W(\omega)\frac{i}{Q_{\rm P}(\omega)} + e(\theta)W(\omega)\frac{i}{Q_{\rm S}(\omega)}, \end{aligned}$$

$$S_{\rm PSV}(\varphi,\omega) = h(\varphi)W(\omega)R_{\rm S} + k(\varphi)W(\omega)R_{\rm D} + l(\varphi)W(\omega)\frac{i}{Q_{\rm S}(\omega)}, \tag{18}$$

where

$$\begin{aligned} a(\theta) &= \sec^2\theta, \\ b(\theta) &= -8g\sin^2\theta, \\ c(\theta) &= 4g\sin^2\theta - \tan^2\theta, \\ d(\theta) &= -\sec^2\theta[R_{\rm P}(\omega) - \frac{1}{2}R_{\rm D} - \frac{1}{4}], \\ e(\theta) &= 4g\sin^2\theta[2R_{\rm S}(\omega) - R_{\rm D} - \frac{1}{2}], \\ h(\varphi) &= -4\frac{\sin\theta}{\cos\varphi}(\sqrt{g}\cos\theta\cos\varphi - g\sin^2\theta), \\ k(\varphi) &= \frac{\sin\theta}{\cos\varphi}(2\sqrt{g}\cos\theta\cos\varphi - 2g\sin^2\theta - 1), \end{aligned}$$

$$l(\varphi) = 2\frac{\sin\theta}{\cos\varphi}(\sqrt{g}\cos\theta\cos\varphi - g\sin^2\theta)[2R_{\rm S}(\omega) - R_{\rm D} - \frac{1}{2}].$$

To found the least square inverse problem, we re-write equation 18 for the case of M interface and N incident angle as

$$\begin{bmatrix} S_{\rm PP}(\theta_1,\omega) \\ \vdots \\ S_{\rm PP}(\theta_N,\omega) \\ S_{\rm PSV}(\varphi_1,\omega) \\ \vdots \\ S_{\rm PSV}(\varphi_N,\omega) \end{bmatrix} = \begin{bmatrix} A(\theta_1,\omega) & B(\theta_1,\omega) & C(\theta_1,\omega) & D(\theta_1,\omega) & E(\theta_1,\omega) \\ \vdots & \vdots & \vdots & \vdots & \vdots \\ A(\theta_N,\omega) & B(\theta_N,\omega) & C(\theta_N,\omega) & D(\theta_N,\omega) & E(\theta_N,\omega) \\ 0 & H(\varphi_1,\omega) & K(\varphi_1,\omega) & 0 & L(\varphi_1,\omega) \\ \vdots & \vdots & \vdots & \vdots & \vdots \\ 0 & H(\varphi_N,\omega) & K(\varphi_N,\omega) & 0 & L(\varphi_N,\omega) \end{bmatrix} \begin{bmatrix} R_{\rm P}(\omega) \\ R_{\rm S}(\omega) \\ R_{\rm D} \\ \frac{1}{Q_{\rm P}(\omega)} \\ \frac{1}{Q_{\rm S}(\omega)} \end{bmatrix}, \tag{19}$$

where

$$\begin{aligned}
S_{\rm PP}(\theta_i,\omega) &= \begin{bmatrix} S^1_{\rm PP}(\theta_i,\omega) & \cdots & S^M_{\rm PP}(\theta_i,\omega) \end{bmatrix}^{\rm T}, \\
A(\theta_i,\omega) &= \textit{diag}\begin{bmatrix} a^1(\theta_i,\omega)W(\omega) & \cdots & a^M(\theta_i,\omega)W(\omega) \end{bmatrix}^{\rm T}, \\
B(\theta_i,\omega) &= \textit{diag}\begin{bmatrix} b^1(\theta_i,\omega)W(\omega) & \cdots & b^M(\theta_i,\omega)W(\omega) \end{bmatrix}^{\rm T}, \\
C(\theta_i,\omega) &= \textit{diag}\begin{bmatrix} c^1(\theta_i,\omega)W(\omega) & \cdots & c^M(\theta_i,\omega)W(\omega) \end{bmatrix}^{\rm T}, \\
D(\theta_i,\omega) &= \textit{diag}\begin{bmatrix} d^1(\theta_i,\omega)W(\omega) & \cdots & d^M(\theta_i,\omega)W(\omega) \end{bmatrix}^{\rm T}, \\
E(\theta_i,\omega) &= \textit{diag}\begin{bmatrix} e^1(\theta_i,\omega)W(\omega) & \cdots & e^M(\theta_i,\omega)W(\omega) \end{bmatrix}^{\rm T}, \\
H(\varphi_i,\omega) &= \textit{diag}\begin{bmatrix} h^1(\varphi_i,\omega)W(\omega) & \cdots & h^M(\varphi_i,\omega)W(\omega) \end{bmatrix}^{\rm T}, \\
K(\varphi_i,\omega) &= \textit{diag}\begin{bmatrix} k^1(\varphi_i,\omega)W(\omega) & \cdots & k^M(\varphi_i,\omega)W(\omega) \end{bmatrix}^{\rm T}, \\
L(\varphi_i,\omega) &= \textit{diag}\begin{bmatrix} l^1(\varphi_i,\omega)W(\omega) & \cdots & l^M(\varphi_i,\omega)W(\omega) \end{bmatrix}^{\rm T}, \\
R_{\rm P}(\omega) &= \begin{bmatrix} R^1_{\rm P}(\omega) & \cdots & R^M_{\rm P}(\omega) \end{bmatrix}^{\rm T}, \\
R_{\rm S}(\omega) &= \begin{bmatrix} R^1_{\rm S}(\omega) & \cdots & R^M_{\rm S}(\omega) \end{bmatrix}^{\rm T}, \\
R_{\rm D} &= \begin{bmatrix} R^1_{\rm D} & \cdots & R^M_{\rm D} \end{bmatrix}^{\rm T}, \\
\frac{1}{Q_{\rm P}(\omega)} &= \begin{bmatrix} \frac{1}{Q^1_{\rm P}(\omega)} & \cdots & \frac{1}{Q^M_{\rm P}(\omega)} \end{bmatrix}^{\rm T}, \\
\frac{1}{Q_{\rm S}(\omega)} &= \begin{bmatrix} \frac{1}{Q^1_{\rm S}(\omega)} & \cdots & \frac{1}{Q^M_{\rm S}(\omega)} \end{bmatrix}^{\rm T}.
\end{aligned}$$

Equation 19 may be succinctly expressed as

$$d = Gm, \tag{20}$$

where d is the offset-dependent seismic data vector, G is the complex frequency-dependent operator, and m is the unknown parameter vector.

Singular value decomposition (SVD) is employed to solve the least-square problem. The matrix can be expressed as a product of three matrices

$$G = U\Lambda V^{\mathrm{T}}, \tag{21}$$

where Λ is a diagonal matrix that consists of the singular values, $U^{\mathrm{T}} = U^{\text{-}1}$, and $V^{\mathrm{T}} = V^{\text{-}1}$.

Therefore, the least squares solution of equation 20 is given by

$$m = (G^{\mathrm{T}}G)^{-1}G^{\mathrm{T}}d = (V\Lambda^{\mathrm{T}}U^{\mathrm{T}}U\Lambda V^{\mathrm{T}})^{-1}V\Lambda^{\mathrm{T}}U^{\mathrm{T}}d = V\Lambda^{-1}U^{\mathrm{T}}d. \tag{22}$$

However, in the case that Λ^{-1} doesn't exist, we can't obtain the least squares solution. Moreover, if there is very small singular value in Λ, Λ^{-1} becomes large and the solution is instable. Here the damped least squares should be used to make the inversion more stable.

$$\begin{aligned} m = (G^{\mathrm{T}}G + \varepsilon^2)^{-1}G^{\mathrm{T}}d &= (V\Lambda^{\mathrm{T}}U^{\mathrm{T}}U\Lambda V^{\mathrm{T}} + \varepsilon^2 VIV^{\mathrm{T}})^{-1}V\Lambda^{\mathrm{T}}U^{\mathrm{T}}d \\ &= V(\Lambda^{\mathrm{T}}\Lambda + \varepsilon^2 I)^{-1}\Lambda^{\mathrm{T}}U^{\mathrm{T}}d.. \end{aligned} \tag{23}$$

In equation 23, we see that the damping factor ε^2 may help to avoid the large value in the inverse of Λ. In other words, for each singular value, λ_i^{-1} , becomes $\lambda_i/(\lambda_i^{-1} + \varepsilon^2)$.

Considering seismic frequency, the low-frequency model (constructed by well-logging data and rock physics analysis results), should be employed, and the iteration is used to get the more accurate inversion results.

$$m = m_{\text{init}} + V(\Lambda^{\mathrm{T}}\Lambda + \varepsilon^2 I)^{-1}\Lambda^{\mathrm{T}}U^{\mathrm{T}}(d - Gm_{\text{init}}), \tag{24}$$

where m_{init} denotes the initial low-frequency model of the unknown parameters.

EXAMPLES

Utilizing the well-logging interpretation results (clay volume V_{C}, porosity Φ and gas saturation S_{g}, Figure 5), we first calculate to the frequency-dependent P- wave and S- wave quality factors with the extension of Mavko-Jizba squirt model. Here we assume that the Z value is 0.08, pore aspect ratio is 0.1, and the effective bulk modulus of dry rock at very high pressure is 50 GPa.

Figure 6 shows the estimated results of P- wave and S- wave velocities and inverse quality factors at different seismic frequencies (20 HZ, 40 HZ, 60 HZ and 80 HZ). We can see that the P- wave and S- wave velocities and inverse quality factors increase with seismic frequency and the changes of quality factors with frequency are larger than the velocities, which may also confirm the variation of real part of reflection coefficient with frequency (Figure 4) is small in seismic frequency range. The corresponding frequency wavelets, which are used to generate synthetic traces, are shown in Figure 5.

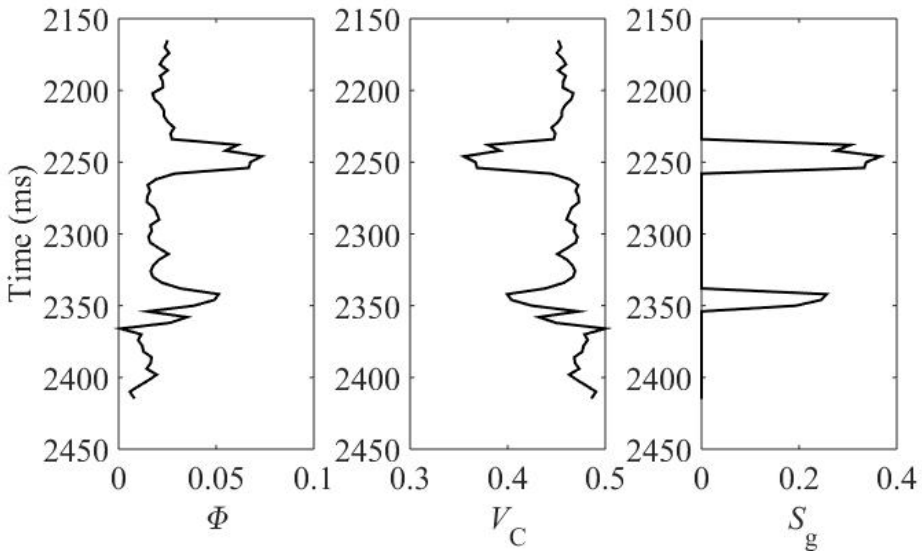

FIG. 5. Well-logging interpretation results.

Figure 8 and Figure 9 show the comparison between inversion results (red) and true values (blue) of P- wave and S- wave impedances, inverse quality factors, and density at different frequencies for the case that the signal to noise ratios are 5 and 2, respectively. The initial models (green) of unknown parameters are the smooth results of the true values. We see that the inversion may obtain the reasonable results of P- wave and S- wave impedances and inverse quality factors when the synthetic data has moderate white Gaussian noise, the results estimated by using the low-frequency (20HZ) synthetic data are smoother than that estimated by utilizing other frequency seismic data, and the accuracy of density inversion should be improved.

CONCLUSIONS

We derive the approximate equations of PP- wave and PSV- wave reflection coefficients in terms of P- wave and S- wave impedances, density, and P- wave and S- wave inverse quality factors. The reflection coefficients consist of two parts: the real part, which shows the effects of elastic properties on reflection coefficients, and the imaginary part, which involves the effects of elastic properties and quality factors. From variations of PP- wave and PSV- wave reflection coefficients with frequency, we find that the effect of frequency on real parts of reflection coefficients is ignorable in seismic frequency range. Therefore, we don't consider the frequency influence on seismic inversion for the elastic properties (P-wave and S-wave impedances, and density).

Using the approximate equations, we demonstrate a method to implement joint inversion of PP- wave and PSV- wave data to estimate the elastic and attenuation parameters for hydrocarbon reservoirs at different frequencies. Interpretation results of well log data are employed to calculate P- wave and S- wave quality factors at different first, and then the calculated results are used to generate the real and imaginary parts of synthetic seismic data to test our method. Tests on synthetic data show that P- wave and S- wave impedances, and inverse quality factors can be estimated reasonably at different frequencies when the

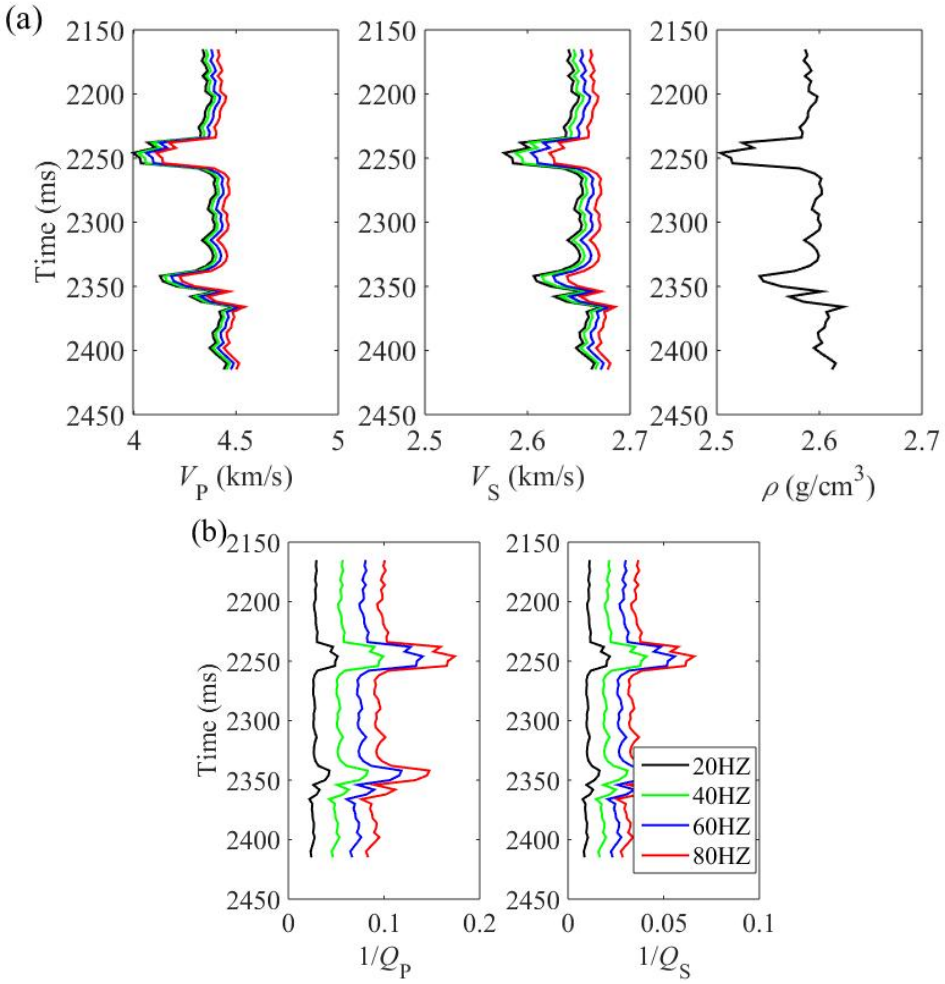

FIG. 6. The estimated results of P- wave and S- wave velocities and inverse quality factors at different seismic frequencies.

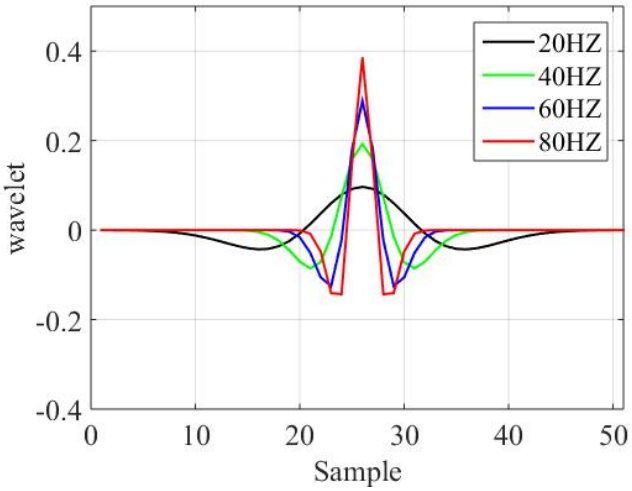

FIG. 7. The corresponding wavelets for generating synthetic seismic data.

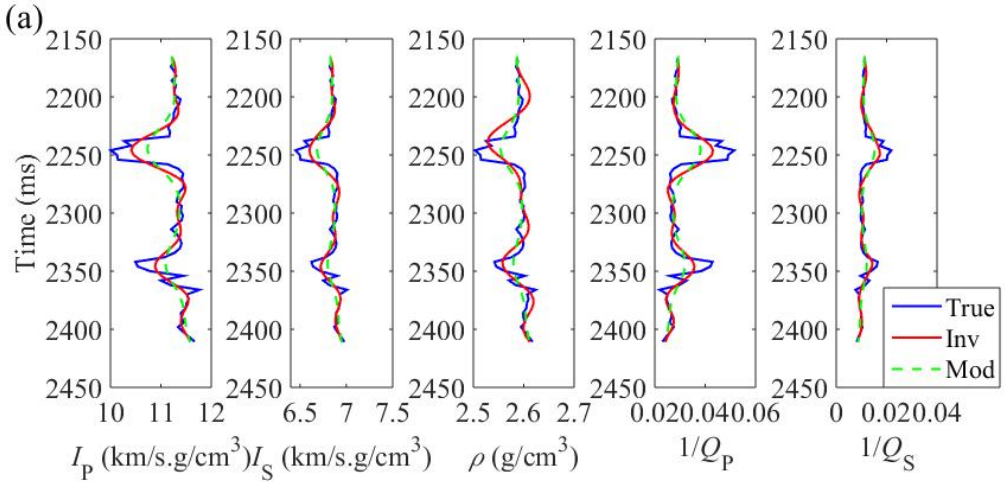
(a)
Time (ms)
2150
2200
2250
2300
2350
2400
2450
10 11 12
6.5 7 7.5
2.5 2.6 2.7
0.02 0.04 0.06
0 0.02 0.04
I_P (km/s.g/cm^3)
I_S (km/s.g/cm^3)
ρ (g/cm^3)
$1/Q_P$
$1/Q_S$
True
Inv
Mod

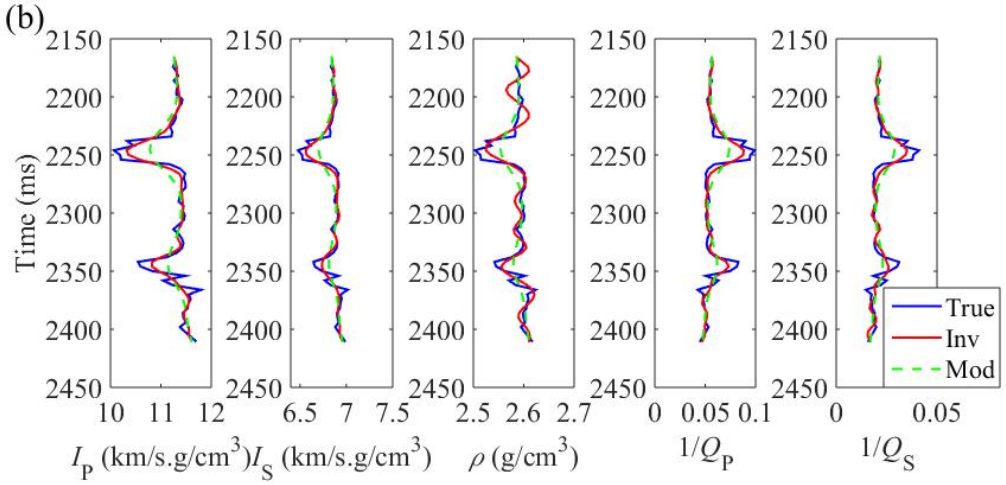
(b)
Time (ms)
2150
2200
2250
2300
2350
2400
2450
10 11 12
6.5 7 7.5
2.5 2.6 2.7
0 0.05 0.1
0 0.05
I_P (km/s.g/cm^3)
I_S (km/s.g/cm^3)
ρ (g/cm^3)
$1/Q_P$
$1/Q_S$
True
Inv
Mod

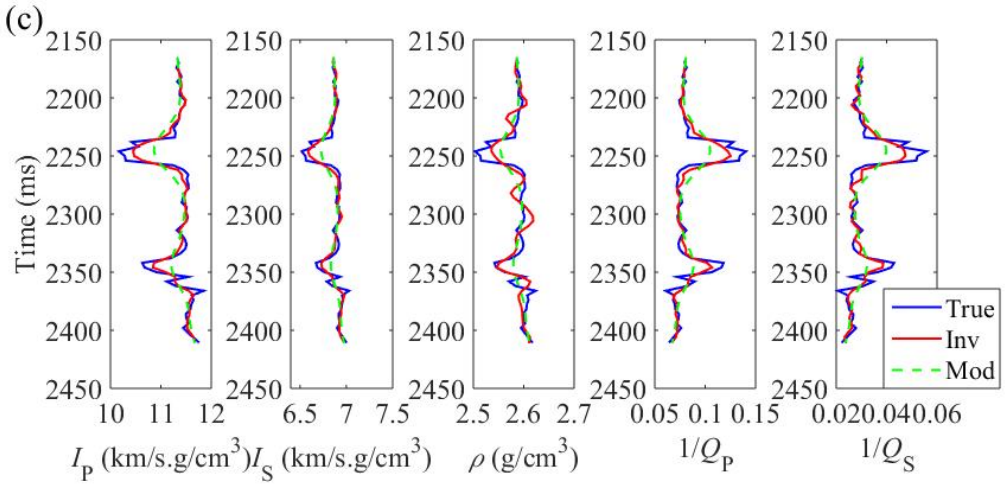
(c)
Time (ms)
2150
2200
2250
2300
2350
2400
2450
10 11 12
6.5 7 7.5
2.5 2.6 2.7
0.05 0.1 0.15
0.02 0.04 0.06
I_P (km/s.g/cm^3)
I_S (km/s.g/cm^3)
ρ (g/cm^3)
$1/Q_P$
$1/Q_S$
True
Inv
Mod

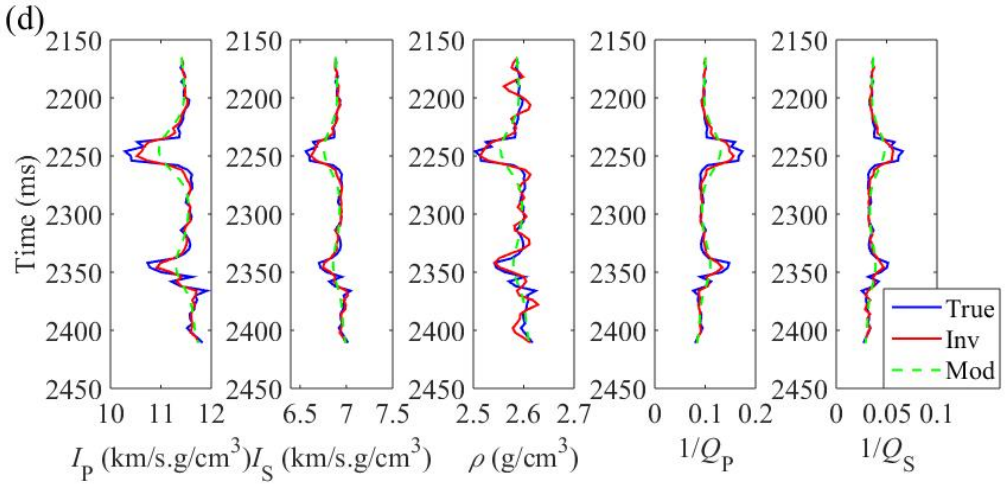

FIG. 8. The comparisons between inversion results (red) and true values (blue) for the case of S/N being 5. The dashed green line represents the initial model. (a) 20HZ, (b) 40HZ, (c) 60 HZ, and (d) 80 HZ.

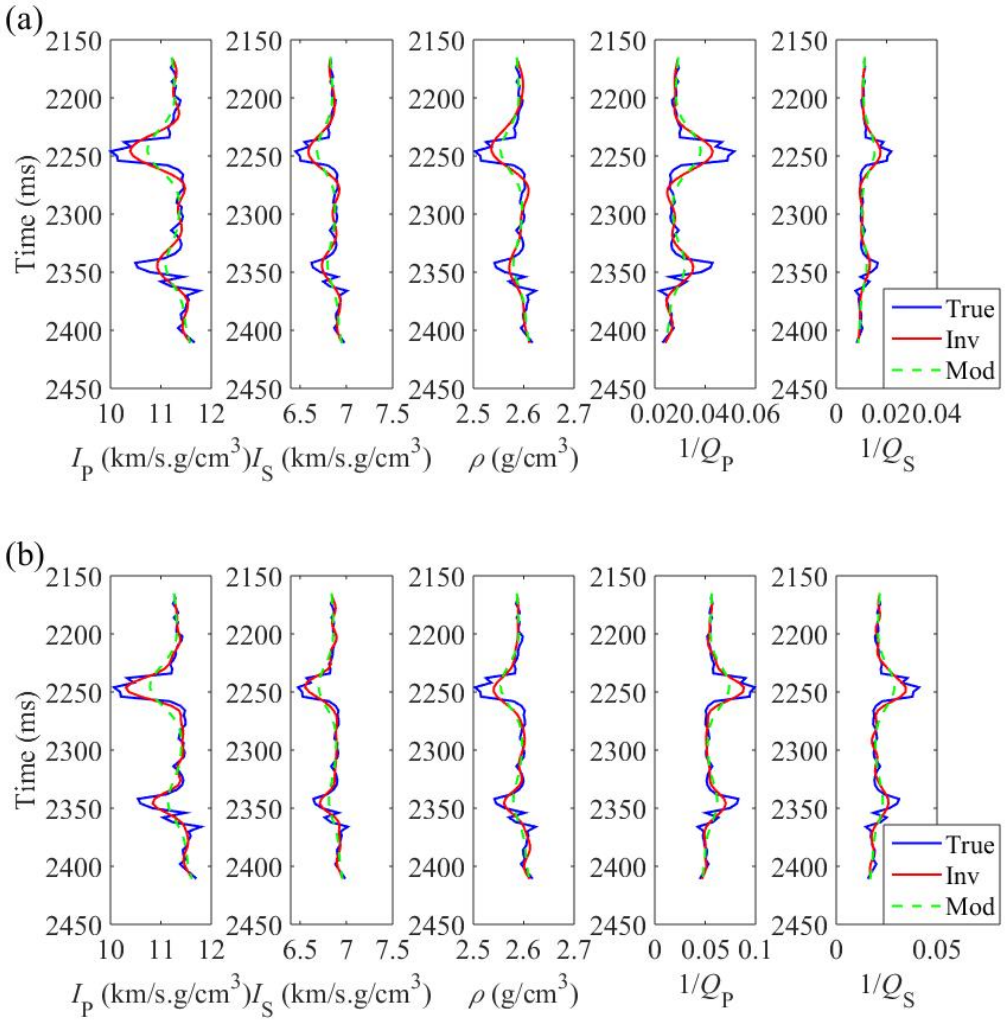

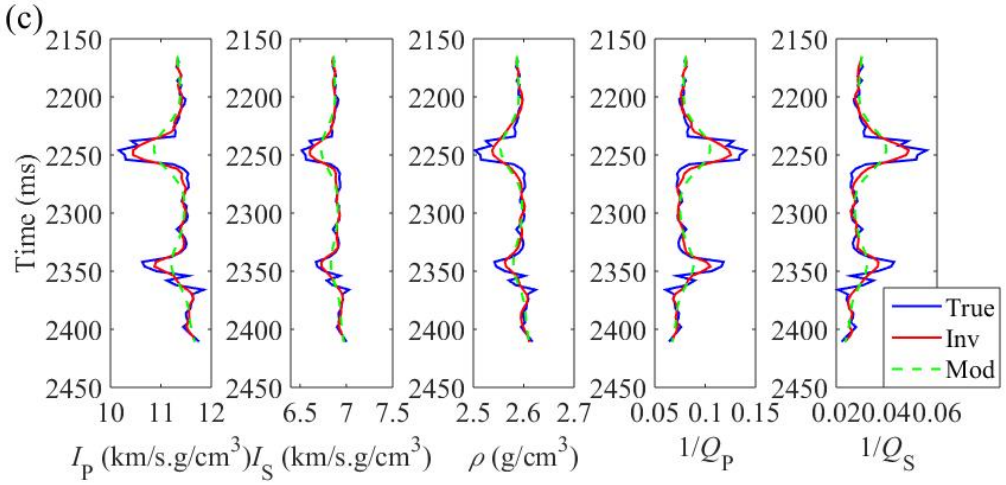

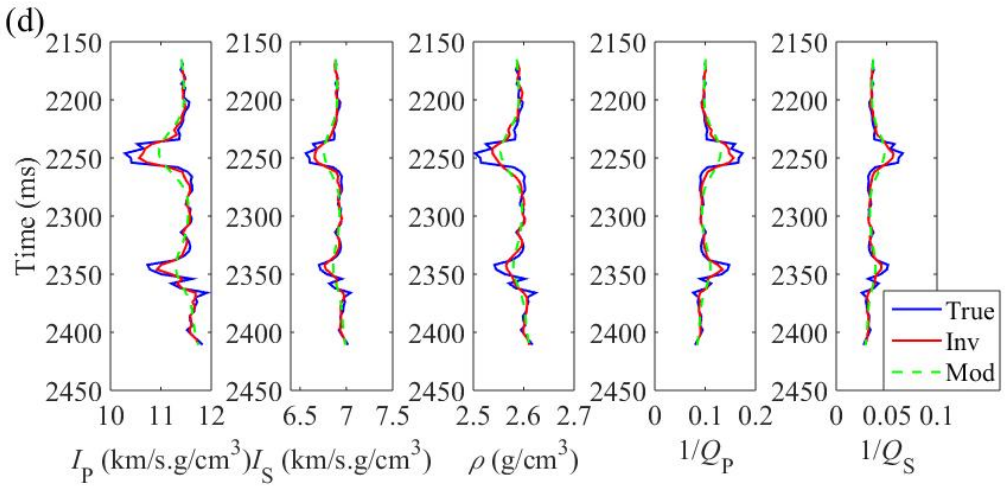

FIG. 9. The comparisons between inversion results (red) and true values (blue) for the case of S/N being 2. The dashed green line represents the initial model. (a) 20HZ, (b) 40HZ, (c) 60 HZ, and (d) 80 HZ.

synthetic data are added with the moderate noise.

The future work is the implementation of joint inversion of PP- wave and PSV- wave real data. One important task is to construct the imaginary parts of real data. However, if we can ignore the imaginary parts of the square results of reflection coefficients, we may calculate the square results of PP- wave and PSV- wave real data first, and then estimate the elastic properties and inverse quality factors with a nonlinear inversion method.

ACKNOWLEDGEMENTS

We thank the sponsors of CREWES for their support. We gratefully acknowledge support from NSERC (Natural Science and Engineering Research Council of Canada). We also thank the support from SINOPEC Key Lab of Multi-Component Seismic Technology.

REFERENCES

Aki, K, and Richards, P. G., 2002, Quantitative seismology: University Science Books.

Biot, M. A., 1956, Theory of propagation of elastic waves in a fluid saturated porous solid: A. Low-frequency range and B. Higher frequency range: J Acoust Soc Am, 28, 168-191.

Bird, C., 2012, Amplitude-variation-with frequency (AVF) analysis of seismic data over anelastic targets: M.Sc. thesis, The University of Calgary.

Dvorkin, J., Mavko, G., and Nur, A., 1995, Squirt flow in fully saturated rocks: Geophysics, 60, 97-107.

Goodway, B., Chen, T., and Downton, J., 1997, Improved AVO fluid detection and lithology discrimination using Lamé petrophysical parameters; $\lambda\rho$, $\mu\rho$, λ/μ fluidstack, from P and S inversions: SEG Technical Program Expanded Abstracts, 183-186.

Innanen, K. A., 2011, Inversion of the seismic AVF/AVA signatures of highly attenuative targets: Geophysics, 76(1), R1-R14.

Larsen, J.A., 1999, AVO inversion by simultaneous P-P and P-S inversion: M.Sc. thesis, The University of Calgary.

Margrave G. F., Stewart, R. R., and Larsen., J., 2001, Joint P-P and P-S seismic inversion: CREWES Research Report , vol. 13.

Mavko, G., Mukerji, T., and Dvorkin, J., 2009, The rock physics handbook-tools for seismic analysis of porous media: Cambridge University Press.

Moradi, S., and Innanen, K. A., 2015, Scattering of homogeneous and inhomogeneous seismic waves in low-loss viscoelastic media: Geophysical Journal International, 202, 1722-1732.

Shaw, R., and Sen, M., 2004, Born integral, stationary phase and linearized reflection coefficients in weak anisotropic media: Geophysical Journal International, 158, 225-238.

Stewart, R.R., 1990, Joint P and P-SV inversion: CREWES Research Report, vol. 3.

Zong, Z., Yin, X., and Wu, G., 2015, Complex seismic amplitude inversion for P-wave and S-wave quality factors: Geophysical Journal International, 202, 564-577.